## Supporting Information to:

# Proton Stabilized Photochemically Reversible E/Z Isomerization of Spiropyrans

L. Kortekaas,[a] J. Chen,[a] D. Jacquemin,[b] and W. R. Browne[a]

[a] Molecular Inorganic Chemistry, Stratingh Institute for Chemistry, Faculty of Mathematics and Natural Sciences, University of Groningen, Nijenborgh 4, 9747AG Groningen, The Netherlands. E-mail: w.r.browne@rug.nl

[b] Chimie Et Interdisciplinarité, Synthèse, Analyse, Modélisation (CEISAM), UMR CNRS no. 6230, BP 92208, Université de Nantes, 2, Rue de la Houssinière, 44322 Nantes Cedex 3, France. E-mail: Denis.Jacquemin@univ-nantes.fr

**Synthesis of SP.** 1,3,3-trimethyl-2-methyleneindoline (612.2 mg, 3.53 mmol) was added dropwise to a solution containing salicylaldehyde (413.3 mg, 3.38 mmol) in 40 mL EtOH followed by refluxing under Argon for 14 h. Evaporation *in vacuo* yielded pink crystals, which upon transfer to a P4 glass filter and extensive washing with ice-cold EtOH with subsequent vacuum filtrations (8 x 3 mL) turned faint pink (492.5 mg, 1.78 mmol, 50 % yield). $^{1}$H NMR ($CD_3CN$, 600 MHz): δ 7.14 (dt, $J_d$ = 1.27 Hz & $J_t$ = 7.65 Hz, 1 H, *b*), 7.12 (m, 1 H, *j*), 7.09 (m, 2 H, *d* and *i*), 6.94 (d, J= 10.25 Hz, 1 H, *h*), 6.84 (dt, $J_d$ = 1.09 Hz & $J_t$ = 7.44 Hz, 1 H, *c*), 6.81 (dt, $J_d$ = 0.90 Hz & $J_t$ = 7.40 Hz, 1 H, *k*), 6.59 (d, J = 8.11 Hz, 1 H, *l*), 6.55 (d, J = 7.73 Hz, 1 H, *a*), 5.75 (d, J = 10.25 Hz, 1 H, *g*), 2.70 (s, 3 H, *m*), 1.26 (s, 3 H, *e/f*), 1.13 (s, 3 H, *e/f*).

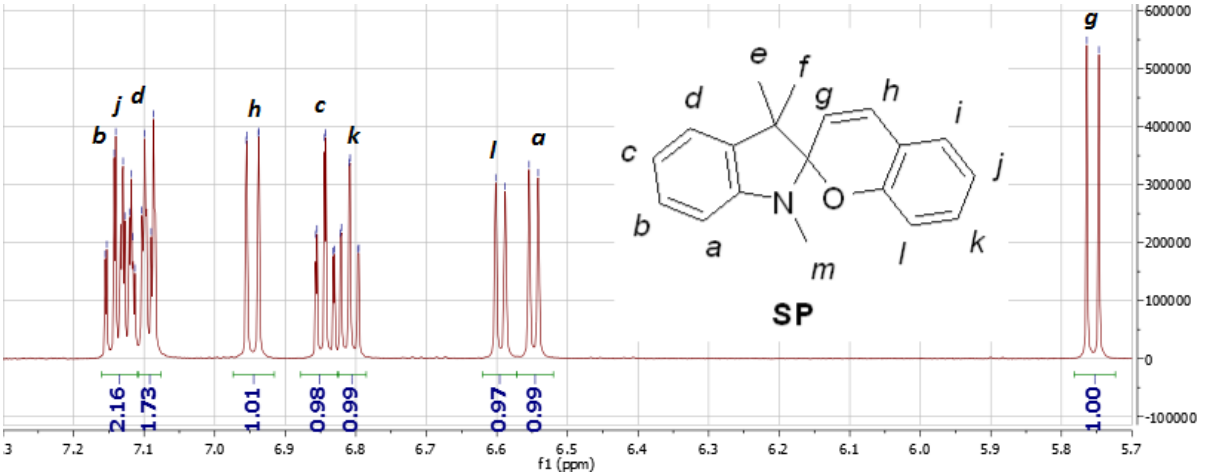


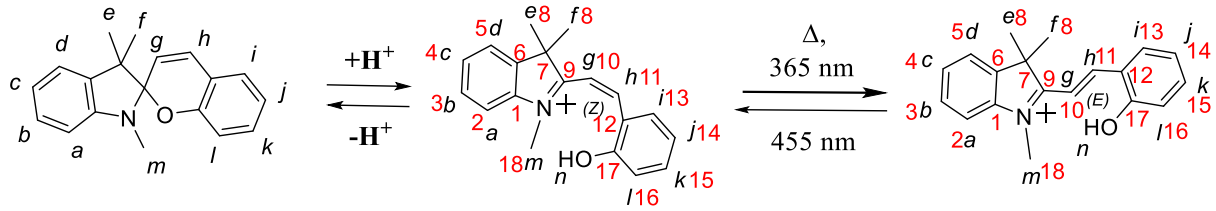


**SP** *Z*-**MCH**$^+$ *E*-**MCH**$^+$

*Z*-**MCH**$^+$ was generated by addition of 1.2 equiv. $CF_3SO_3H$. $^{1}$H NMR of *Z*-**MCH**$^+$ ($CD_3CN$, 600 MHz): δ 7.81 (s, 1 H, *n*), 7.73 (d, J = 7.08 Hz, 1 H, *d*), 7.64 (m, 4 H, *a/b/c/g*), 7.36 (dt, $J_d$ = 1.47 Hz & $J_t$ = 7.76 Hz, 1 H, *j*), 7.21 (dd, J = 1.21 Hz & J = 7.78 Hz, 1 H, *i*), 6.96 (dt, $J_d$ = 0.80 Hz & $J_t$ = 7.54 Hz, 1 H, *k*), 6.90 (d, J = 8.20 Hz, 1 H, *l*), 6.66 (d, J = 12.82 Hz, 1 H, *h*), 3.30 (s, 3 H, *m*), 1.64 (s, 6 H, *e/f*). $^{13}$C APT NMR ($CD_3CN$, 600 MHz): δ *~190.5* (from HMBC, 9), 155.72 (12), 145.60 (10), *~142.8* (from HMBC also, 6 and 1), 133.65 (14), 132.31 (13), 130.59 (2 [or 3]), 129.85 (3 [or 2]), 123.73 (5), 122.90 (17), 121.43 (15), 116.85 (16), 115.97 (4), 112.57 (11), 54.76 (7), 36.81 (18), 23.30 (8).

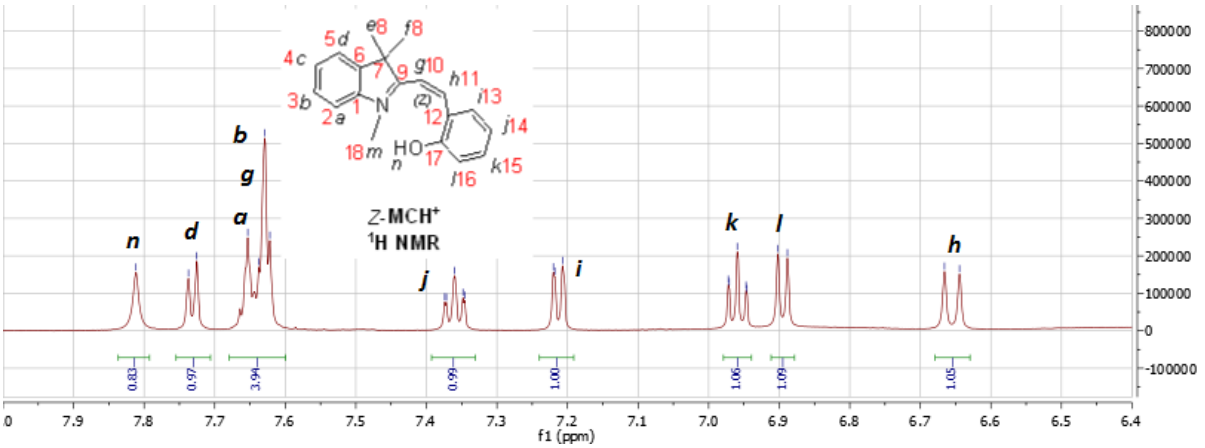
Z-MCH+
1H NMR
n
a
b
g
d
j
i
k
l
h
f1 (ppm)

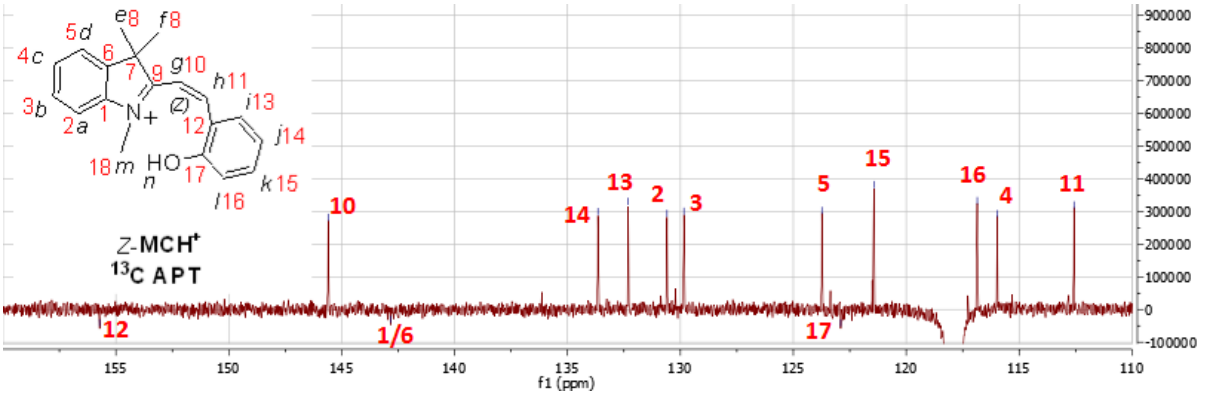
Z-MCH+
13C APT
10
14
13
2
3
5
15
16
4
11
12
1/6
17
f1 (ppm)

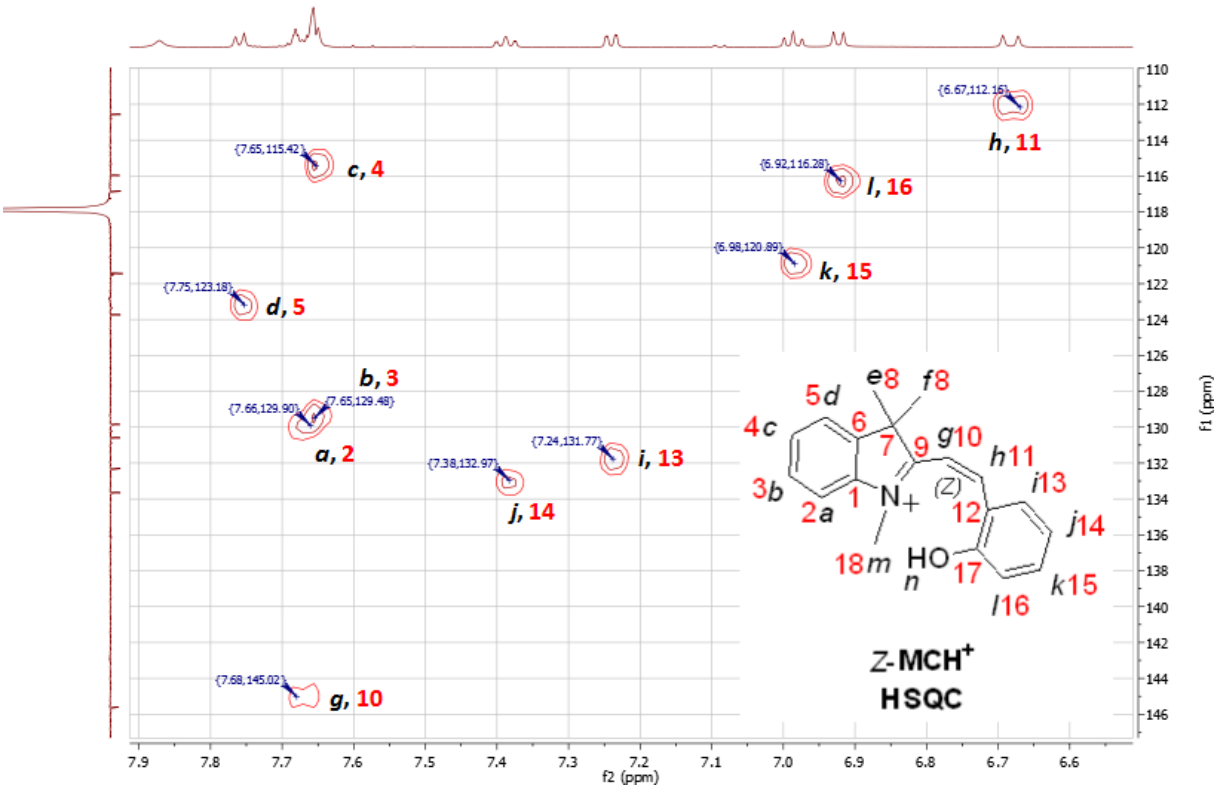
{6.67,112.16}
h, 11
{7.65,115.42}
c, 4
{6.92,116.28}
l, 16
{6.98,120.89}
k, 15
{7.75,123.18}
d, 5
b, 3
{7.66,129.90}
{7.65,129.48}
a, 2
{7.24,131.77}
i, 13
{7.38,132.97}
j, 14
{7.68,145.02}
g, 10
Z-MCH+
HSQC
f2 (ppm)
f1 (ppm)

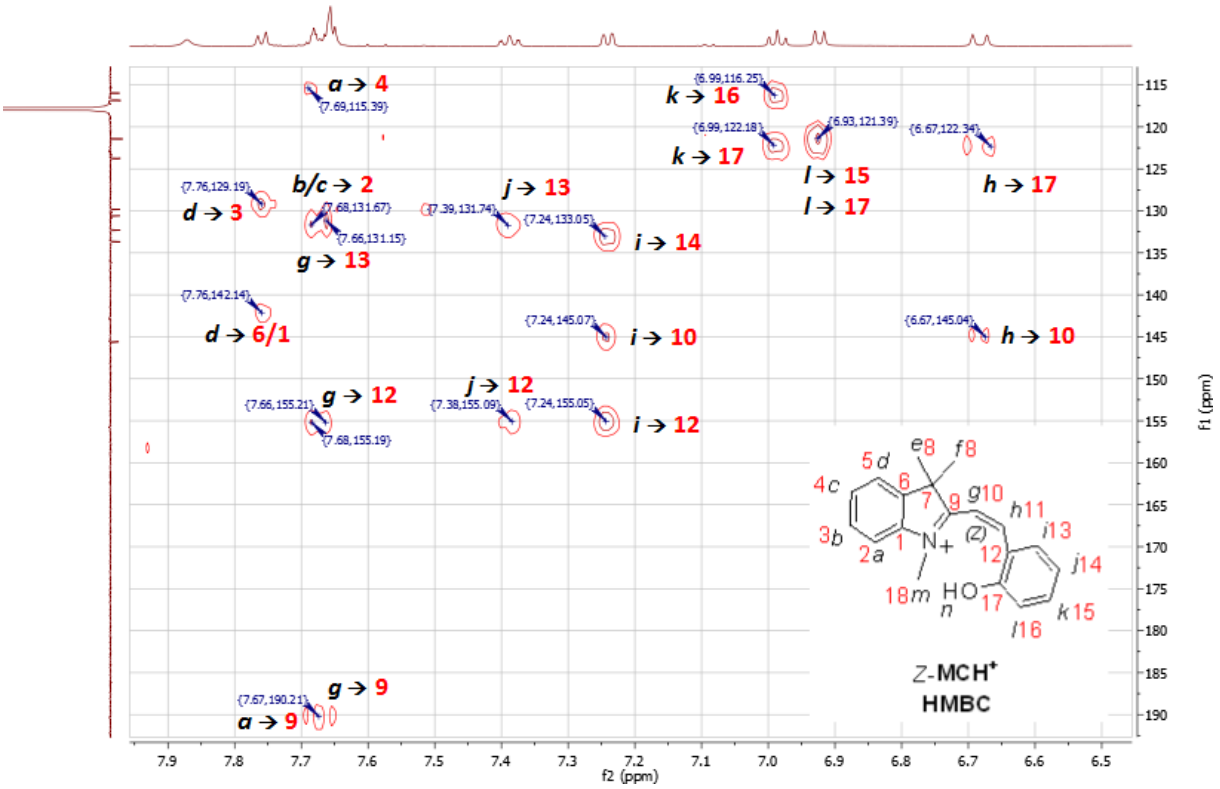
a → 4
{7.69,115.39}
k → 16
{6.99,116.25}
k → 17
{6.99,122.18}
{6.93,121.39}
{6.67,122.34}
l → 15
l → 17
h → 17
{7.76,129.19}
d → 3
b/c → 2
{7.68,131.67}
{7.66,131.15}
g → 13
j → 13
{7.39,131.74}
{7.24,133.05}
i → 14
{7.76,142.14}
d → 6/1
{7.24,145.07}
i → 10
{6.67,145.04}
h → 10
g → 12
{7.66,155.21}
{7.68,155.19}
j → 12
{7.38,155.09}
{7.24,155.05}
i → 12
g → 9
{7.67,190.21}
a → 9
Z-MCH+
HMBC
f2 (ppm)
f1 (ppm)

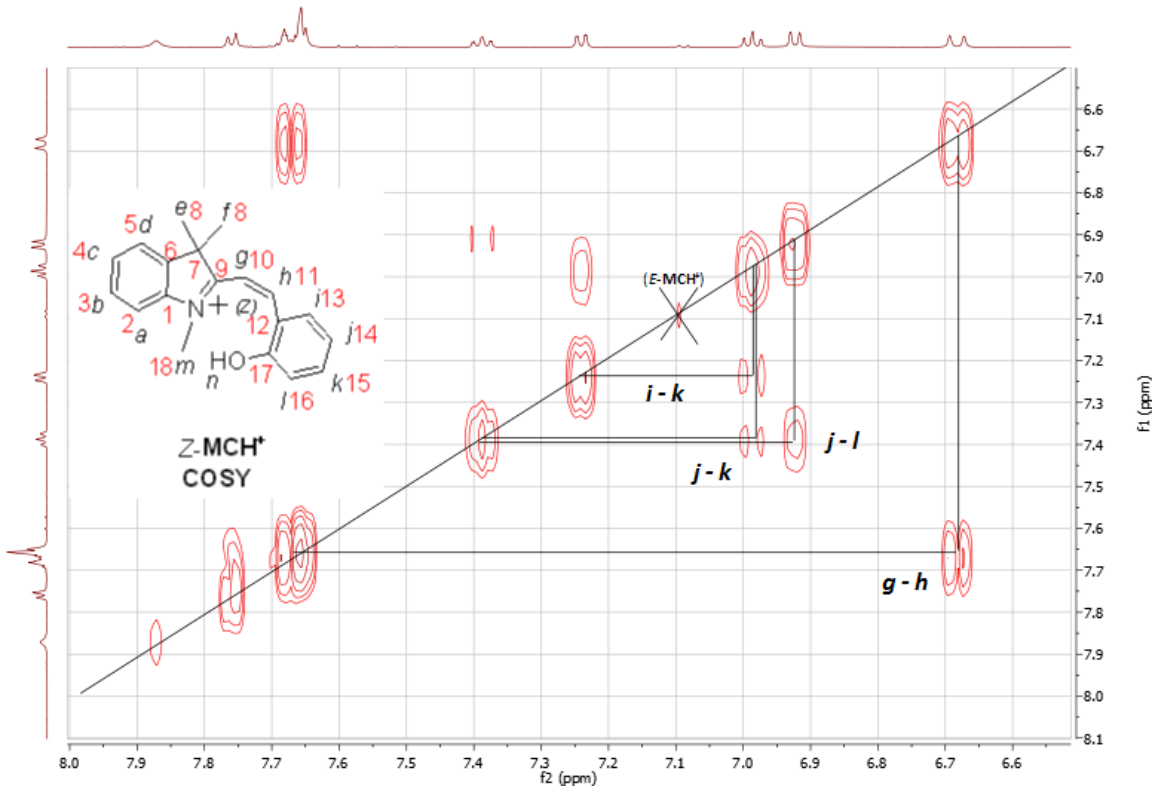
(E-MCH+)
i - k
j - l
j - k
g - h
Z-MCH+
COSY
f2 (ppm)
f1 (ppm)

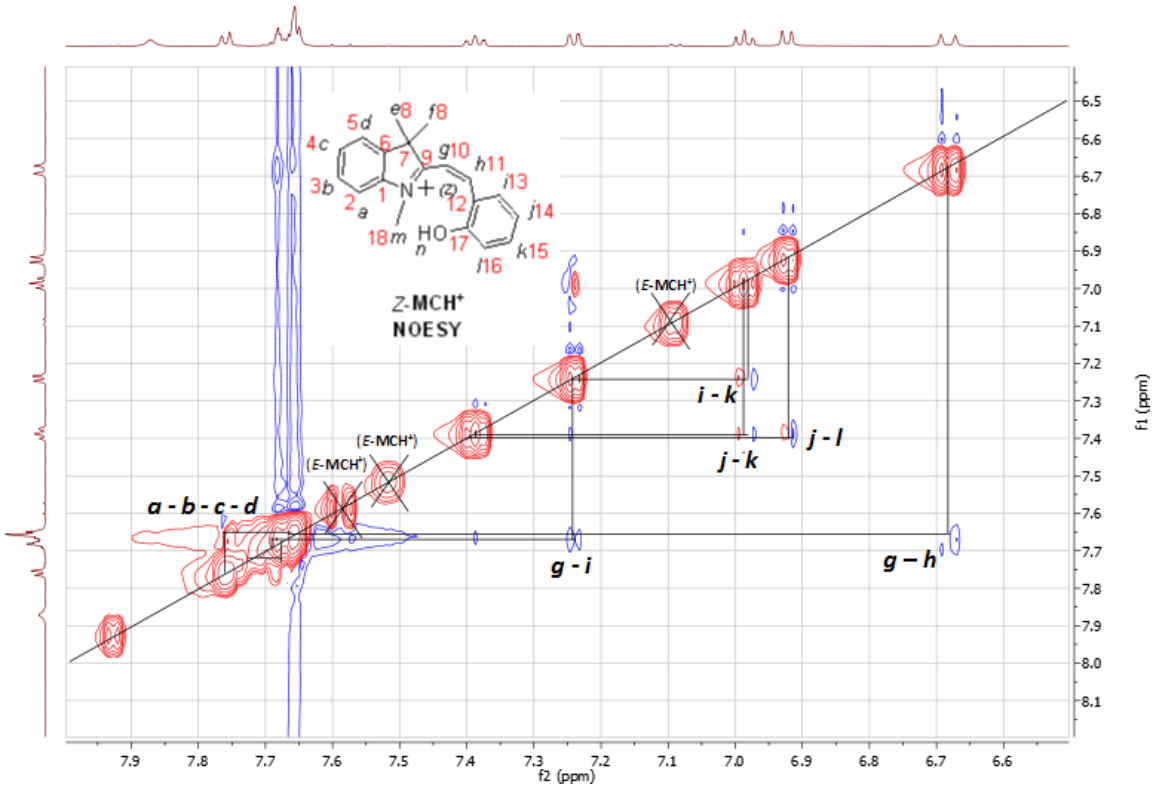


*E*-**MCH**$^+$ was generated by addition of 4 equiv. $PO_4H_3$, , with subsequent thermal equilibration directly to the *E*-form over 48 h. $^1$H NMR ($CD_3CN$, 600 MHz): δ 8.52 (d, J = 16.43 Hz, 1 H, *g*), 7.89 (dd, J = 7.79 Hz and 1.57 Hz, 1 H, *i*), 7.71 (m, 1H, *d*), 7.68 (m, 1H, *c*), 7.63 (m, 1H, *b*), 7.62 (m, 1H, *a*) 7.57 (d, J = 16.43 Hz, 1 H, *h*), 7.49 (dt, $J_d$ = 1.64 Hz, $J_t$ = 7.76 Hz, 1 H, *j*), 7.07 (d, J ≈ 7.71 Hz, 1 H, *l*), 7.06 (t, J ≈ 7.80 Hz, 1 H, *k*), 3.99 (s, 3H, *m*), 1.77 (s, 6H, *e*/*f*). $^{13}$C APT NMR ($CD_3CN$, 600 MHz): δ 183.73 (9), 159.45(12), 150.67 (10), 144.27 (6), 142.85 (1), 136.52 (14), 131.29 (13), 130.58 (2), 130.25 (3), 123.73 (5), 122.30 (17), 121.83 (15), 117.69 (16), 115.69 (4), 113.16 (11), 53.36 (7), 35.11 (18), 26.56 (8).

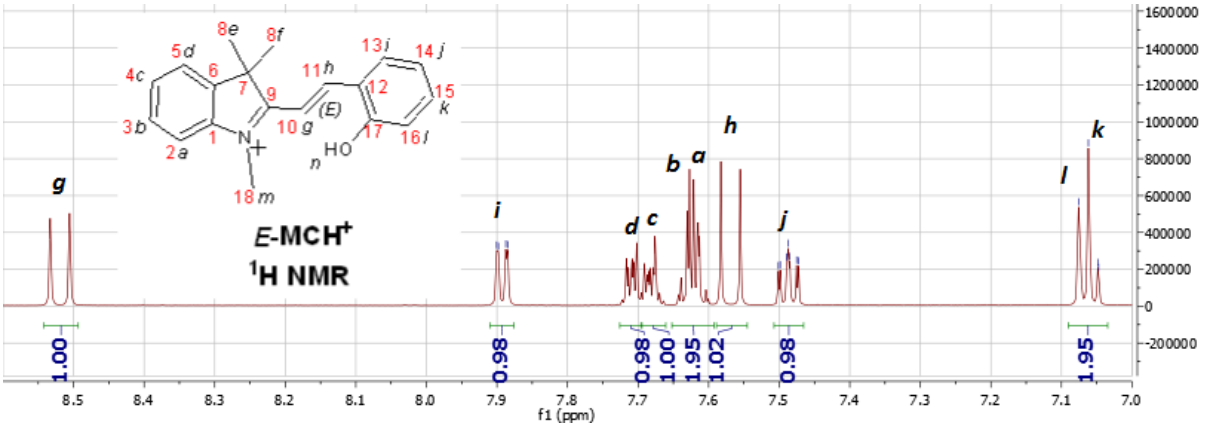

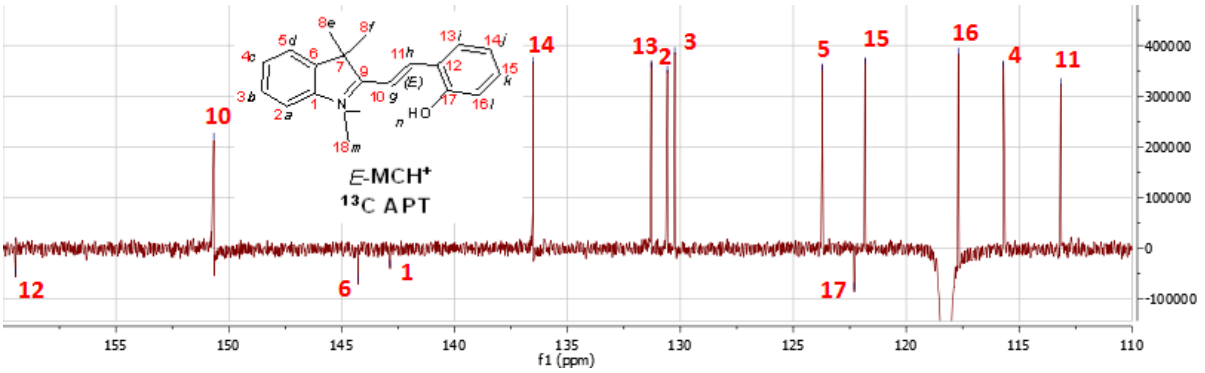
E-MCH+
13C APT
10
14
13
2
3
5
15
16
4
11
12
6
1
17
f1 (ppm)

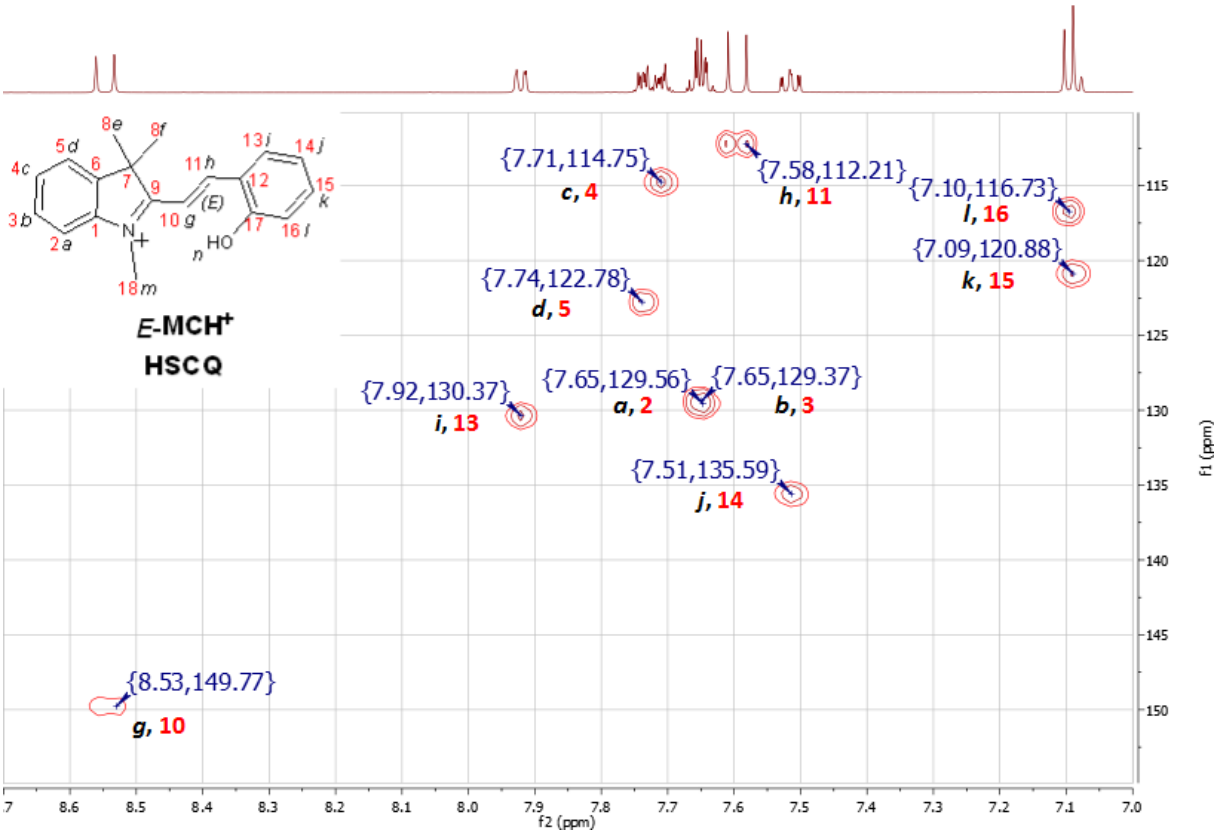
E-MCH+
HSCQ
{7.71,114.75}
c, 4
{7.58,112.21}
h, 11
{7.10,116.73}
l, 16
{7.09,120.88}
k, 15
{7.74,122.78}
d, 5
{7.92,130.37}
i, 13
{7.65,129.56}
a, 2
{7.65,129.37}
b, 3
{7.51,135.59}
j, 14
{8.53,149.77}
g, 10
f2 (ppm)
f1 (ppm)

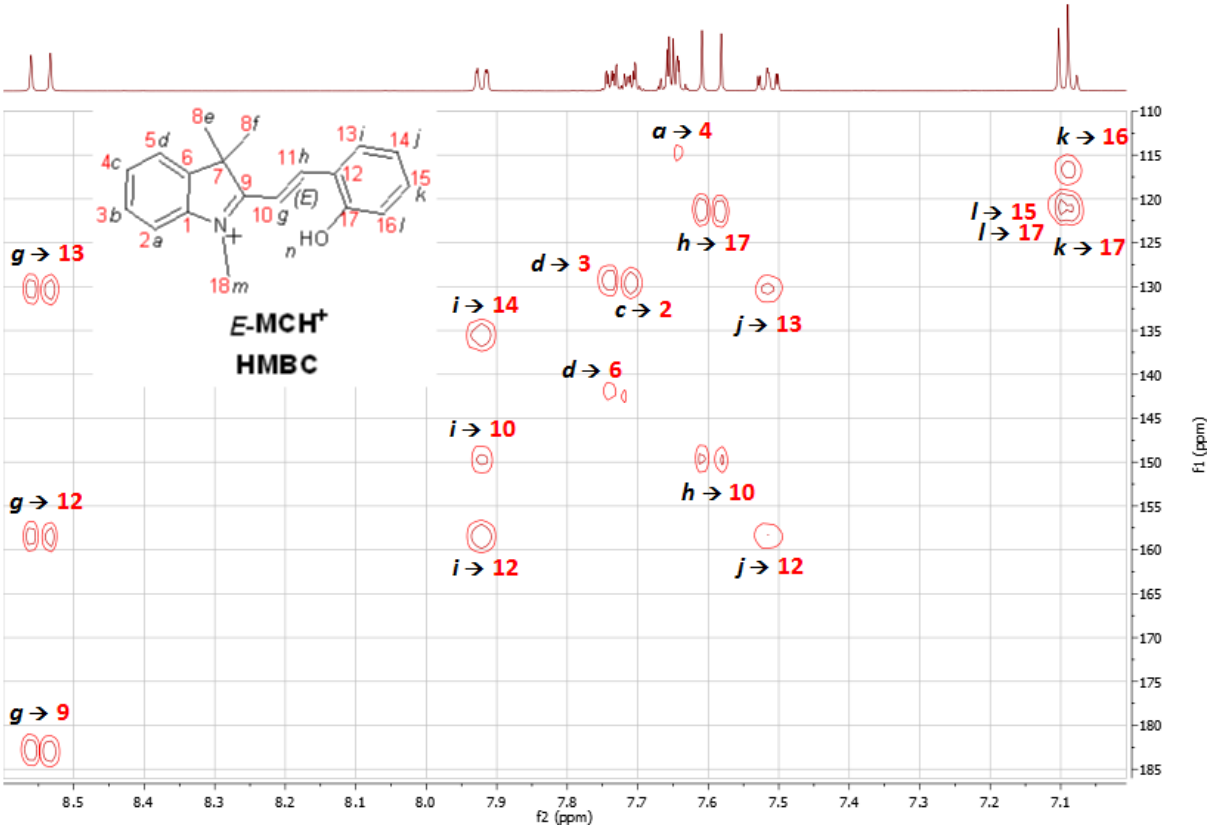
E-MCH+
HMBC
a → 4
k → 16
l → 15
l → 17
k → 17
h → 17
d → 3
g → 13
i → 14
c → 2
j → 13
d → 6
i → 10
h → 10
g → 12
i → 12
j → 12
g → 9
f2 (ppm)
f1 (ppm)

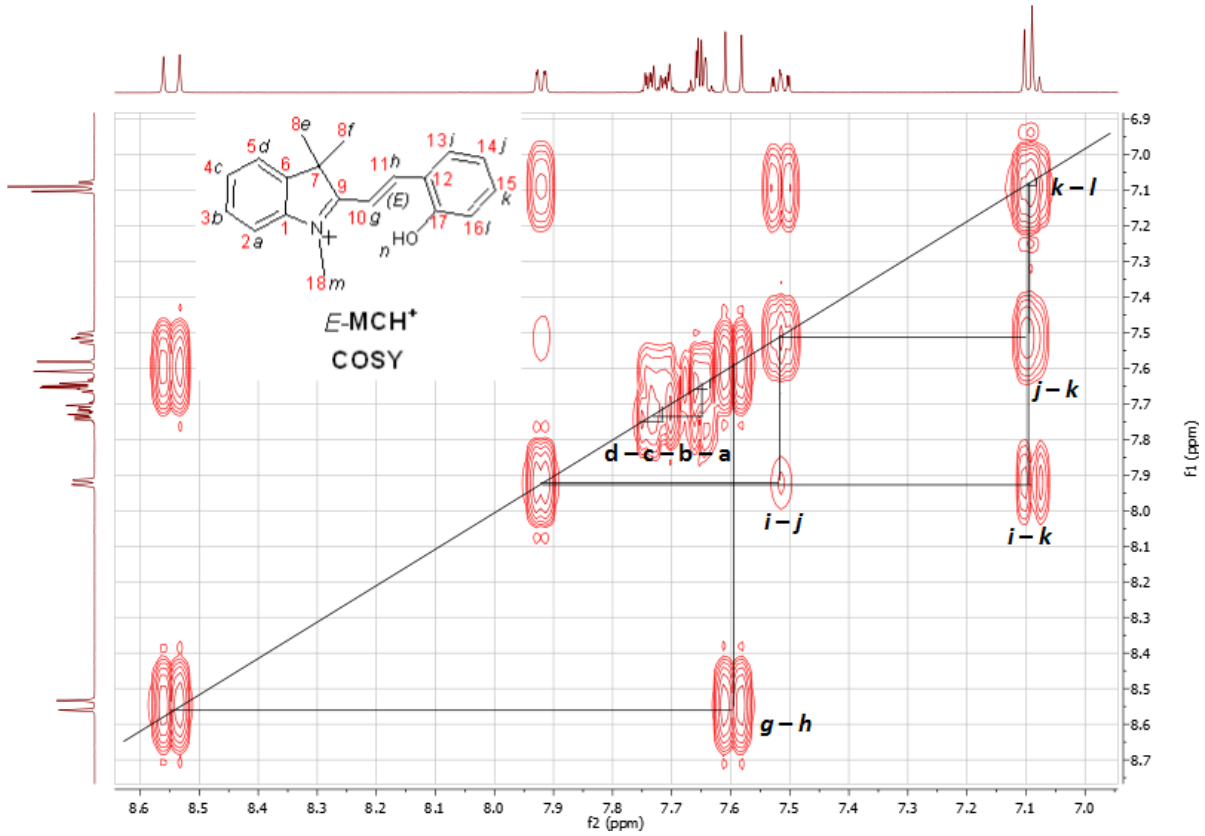
E-MCH+
COSY
k – l
j – k
d – c – b – a
i – j
i – k
g – h
f2 (ppm)
f1 (ppm)

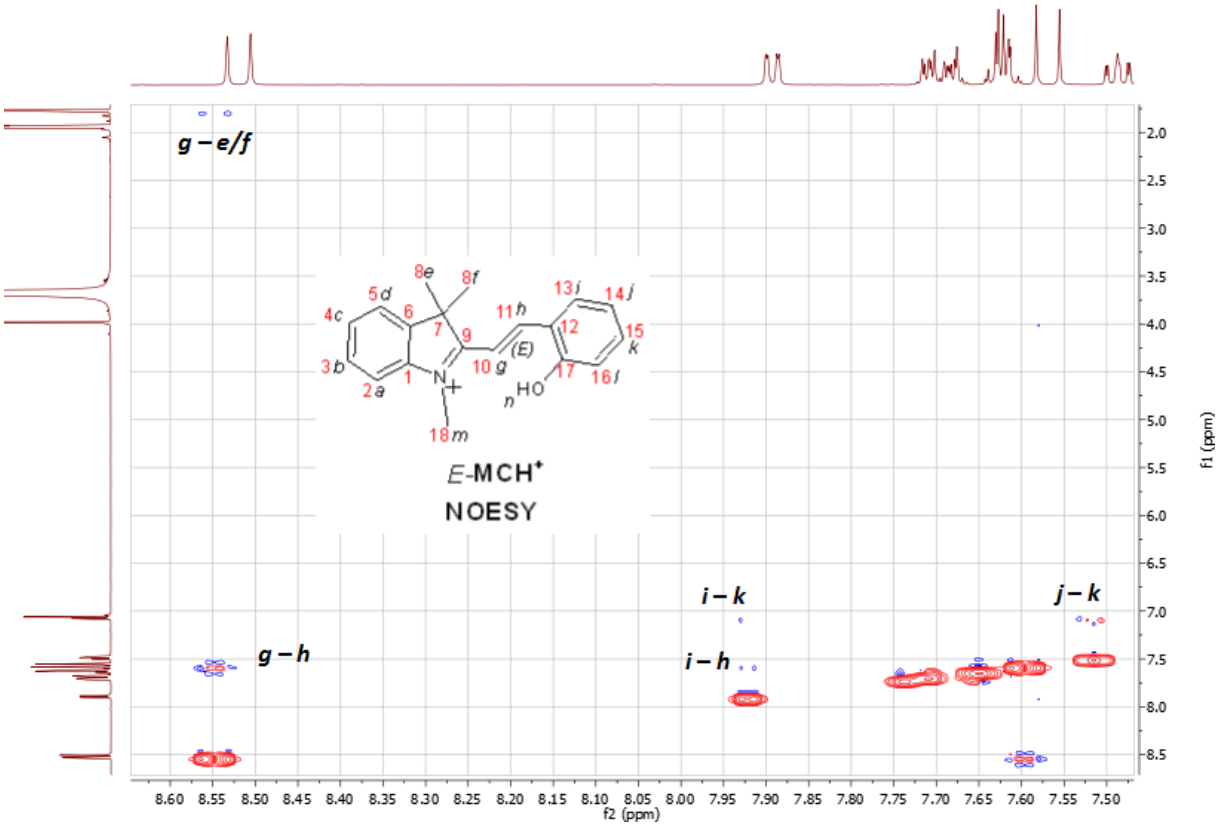
g – e/f
g – h
i – k
i – h
j – k
E-MCH+
NOESY
f2 (ppm)
f1 (ppm)

**Actinometry.** Absolute quantum yields were determined with reference to the actinometer potassium ferrioxalate.[1] Light flux was determined by the method of total absorption using 2 mL of 6 mM (at 355 nm) and 0.15 M (at 457 nm) potassium ferrioxalate in a 1 cm pathlength cuvette with stirring. The actinometer was irradiated for 90 s (at 355 nm) and 45 s (at 457 nm), respectively. A reference cuvette was held apart from the excitation source. After irradiation, 1 mL of each solution was added to buffered aqueous phenanthroline (0.1 M, 2 mL), and diluted 10 fold with water and left to stand in the dark for at least 30 min and the absorbance determined at 510 nm. The photon flux was calculated using equation (e1):

$$(Nhv/t) = \frac{\Delta A}{L \times \varepsilon \times \Phi \times t \times F} \times 20 \quad \text{(E1)}$$

Where L is the pathlength of the cuvette, ε is the molar absorptivity of iron(II) tris-phenanthroline (11100 L mol$^{-1}$ cm$^{-1}$ at $\lambda_{max}$ 510 nm), Φ is quantum yield of the actinometer at 355 nm and 457 nm,[6] t is the irradiation time, F is the fraction of the light the actinometer absorbed.

*Quantum yield theory.*

The trans-to-cis isomerization was calculated as previously reported.[2]

$$-V\frac{dC_1}{dt} = \phi_1 \frac{\varepsilon_1 C_1}{D} \mathrm{I}(1 - 10^{-D}) - \phi_2 \frac{\varepsilon_2 C_2}{D} \mathrm{I}(1 - 10^{-D}) \quad \text{(E2)}$$

$-V\frac{\mathrm{d}C_1}{\mathrm{dt}}$ is the change of species A in mole, $\mathrm{I}(1 - 10^{-\mathrm{D}})$, the light absorbed by the whole system, $\frac{\varepsilon_1 C_1}{D}$ is the fraction of the light absorbed by A, $C_1$, $C_2$ are the concentration of trans and cis isomers, M, $\varepsilon_1$, $\varepsilon_2$ is absorption coefficient of trans and cis isomers at $\lambda_{irri,}$ D is absorbance when using 1 cm path length cuvette, $\phi_1, \phi_2$ are quantum yields for reaction from trans to cis, and cis to trans, I is photon flux determined by actinometry.

Using mole fractions $X = \frac{C}{C_0}$, $C_0 = C_1 + C_2$ is the total concentration, defining $K = \varepsilon_1\phi_1 + \varepsilon_2\Phi_2$,

$$-\frac{dX_1}{dt} \cdot \frac{D}{1-10^{-D}} = \frac{I}{V}\left(\mathrm{KX}_1 - \frac{\varepsilon_2 C_2}{C_0}\right) \quad \text{(E3)}$$

Using $R=\frac{\varepsilon_2 C_2}{C_0}$,

$$\frac{dX_1}{dt} \cdot \frac{D}{1-10^{-D}} = \frac{I}{V}(\mathrm{KX}_1 - R) \quad \text{(E4)}$$

Using $f=\int_0^t \frac{1-10^{-D}}{D} dt$, and integrated the equation, then

$$\ln\frac{(KX_1 - R)}{(KX_0 - R)} = f\frac{KI}{V} \quad \text{(E5)}$$

[1] Hatchard, C.; Parker, C. A. *Proceedings of the Royal Society of London. Series A. Mathematical and Physical Sciences* **1956**, *235*, 518.
[2] Malkin, S.; Fischer, E. *The Journal of Physical Chemistry* **1962**, *66*, 2482.

If to the photostationary state is reached, $\frac{dX_1}{dt}$=0,

$$\left(\mathrm{KX_1} - \frac{\varepsilon_2 C_2}{C_0}\right)=0, \quad \mathrm{KX_1^{\infty}}=\mathrm{R}$$

So,

$$\ln\frac{(\mathrm{KX_1}-\mathrm{KX_1^{\infty}})}{(\mathrm{KX_1^{0}}-\mathrm{KX_1^{\infty}})}=\mathrm{f}\,\frac{KI}{V}, \quad \ln\frac{(\mathrm{X_1}-\mathrm{X_1^{\infty}})}{(\mathrm{X_1^{0}}-\mathrm{X_1^{\infty}})}=\mathrm{f}\,\frac{KI}{V},$$

at photostationary state,

$$-V\frac{dC_1}{dt} = \phi_1 \frac{\varepsilon_1 C_1}{D}\mathrm{I}(1-10^{-D}) - \phi_2 \frac{\varepsilon_2 C_2}{D}\mathrm{I}(1-10^{-D}) = 0$$

$$\varepsilon_1 \phi_1 \mathrm{X_1^{\infty}} = \varepsilon_2 \phi_2 \mathrm{X_2^{\infty}}$$

because $\mathrm{K} = \varepsilon_1\phi_1 + \varepsilon_2\Phi_2$,

$$\emptyset_1=\mathrm{K}\frac{\mathrm{X_2^{\infty}}}{\varepsilon_1},\ \emptyset_2=\mathrm{K}\frac{\mathrm{X_1^{\infty}}}{\varepsilon_2}, \qquad \text{(E6)}$$

**Supporting Figures.**

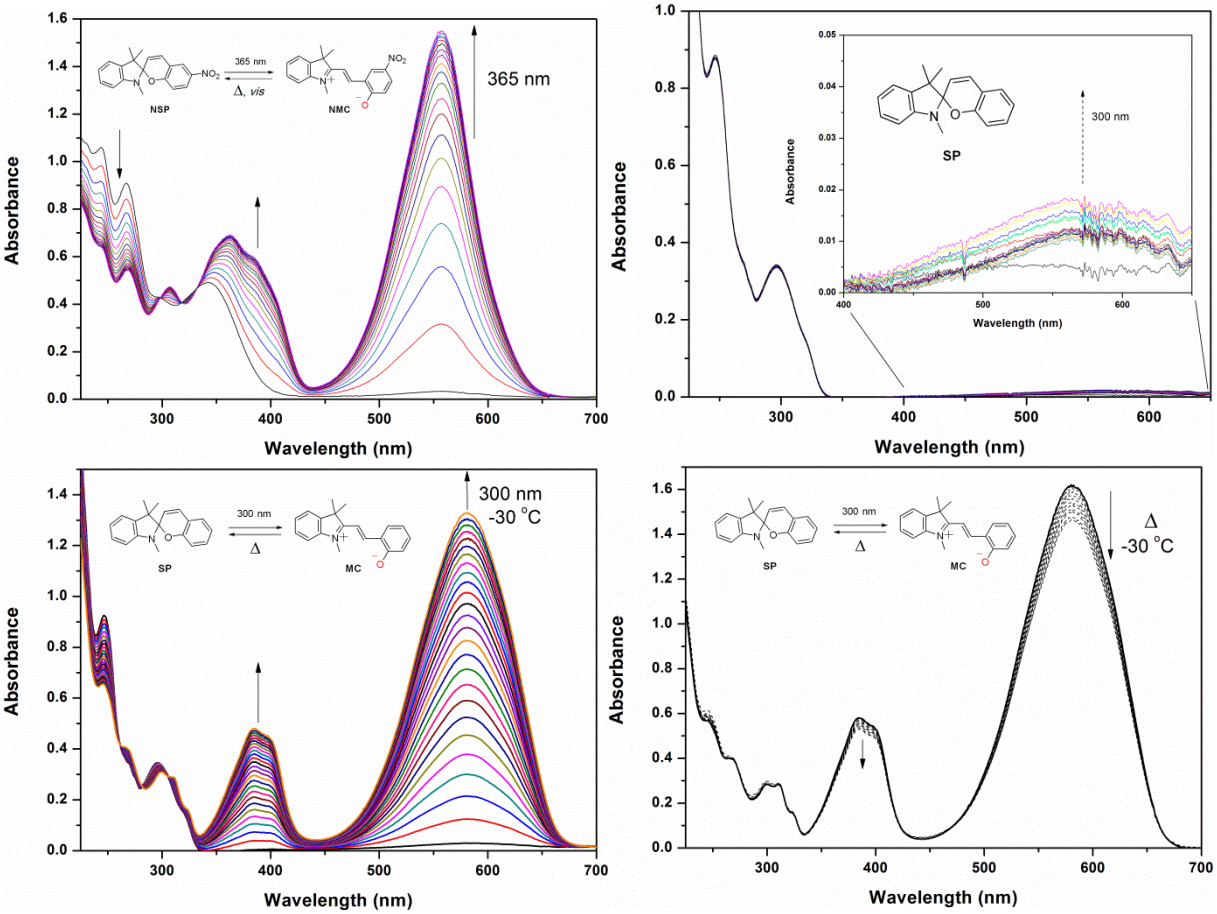


**Figure S1.** (Top left) UV/vis absorption of **NSP** (52 mM in acetonitrile) upon irradiation at 365 nm. (Top right) UV/vis absorption of **SP** (62 mM in acetonitrile) upon irradiation at 300 nm at room temperature (5 s intervals), (bottom left) at -30 °C (100 s intervals) and (bottom right) its subsequent thermal ring closing at -30 °C (100 s intervals) with no observed photoacceleration of the ring closing by irradiation at 565 nm nor 660 nm.

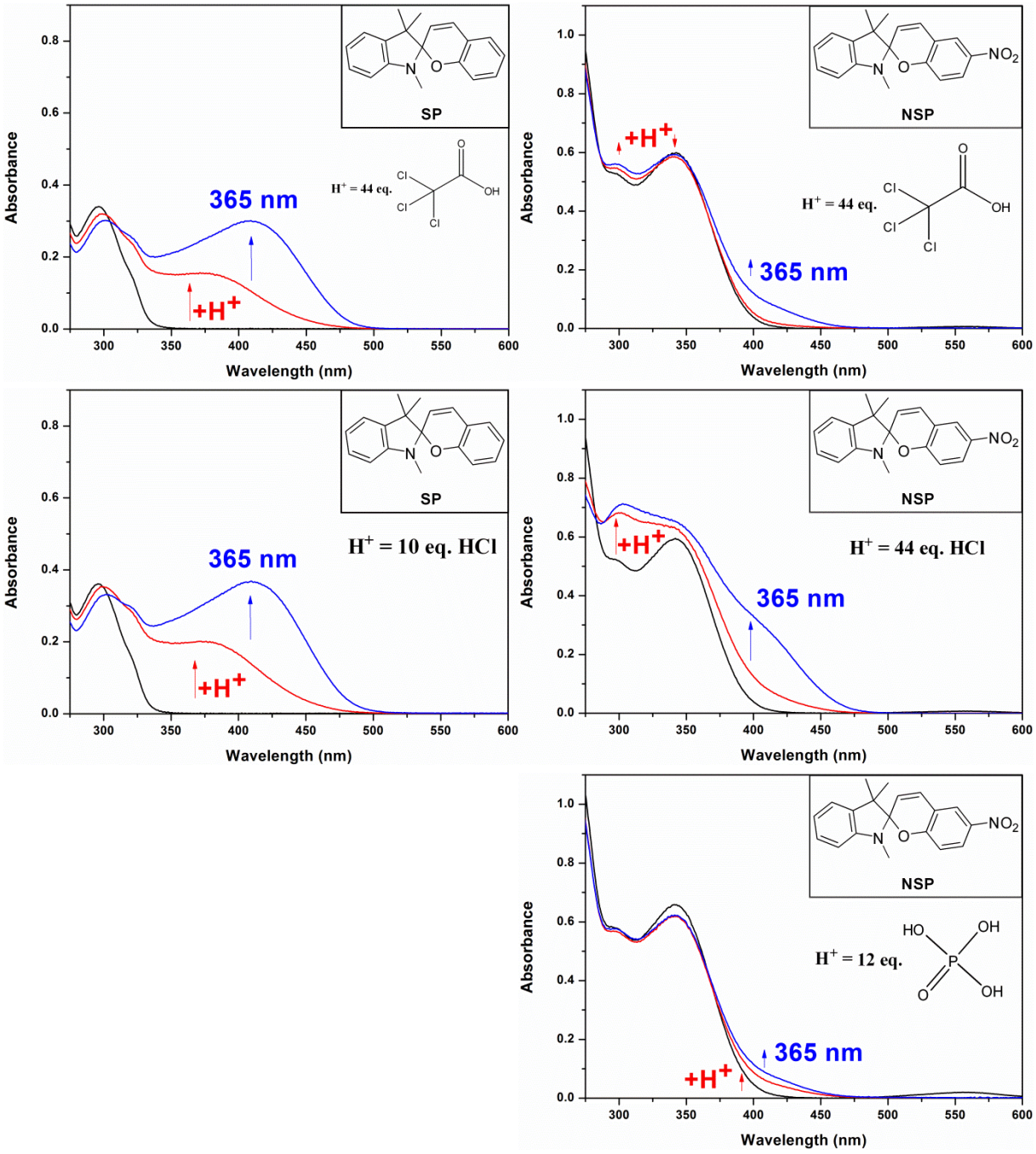


**Figure S2.** UV/vis absorption spectra of 62 µM **SP** (left column) and **NSP** (right column) in acetonitrile (black lines) upon addition of the indicated proton source (red lines) and after subsequent irradiation at 365 nm (blue lines). Reversion to the *Z*-**MCH**$^+$ and *Z*-**NMCH**$^+$ forms is observed upon irradiation at 455 nm.

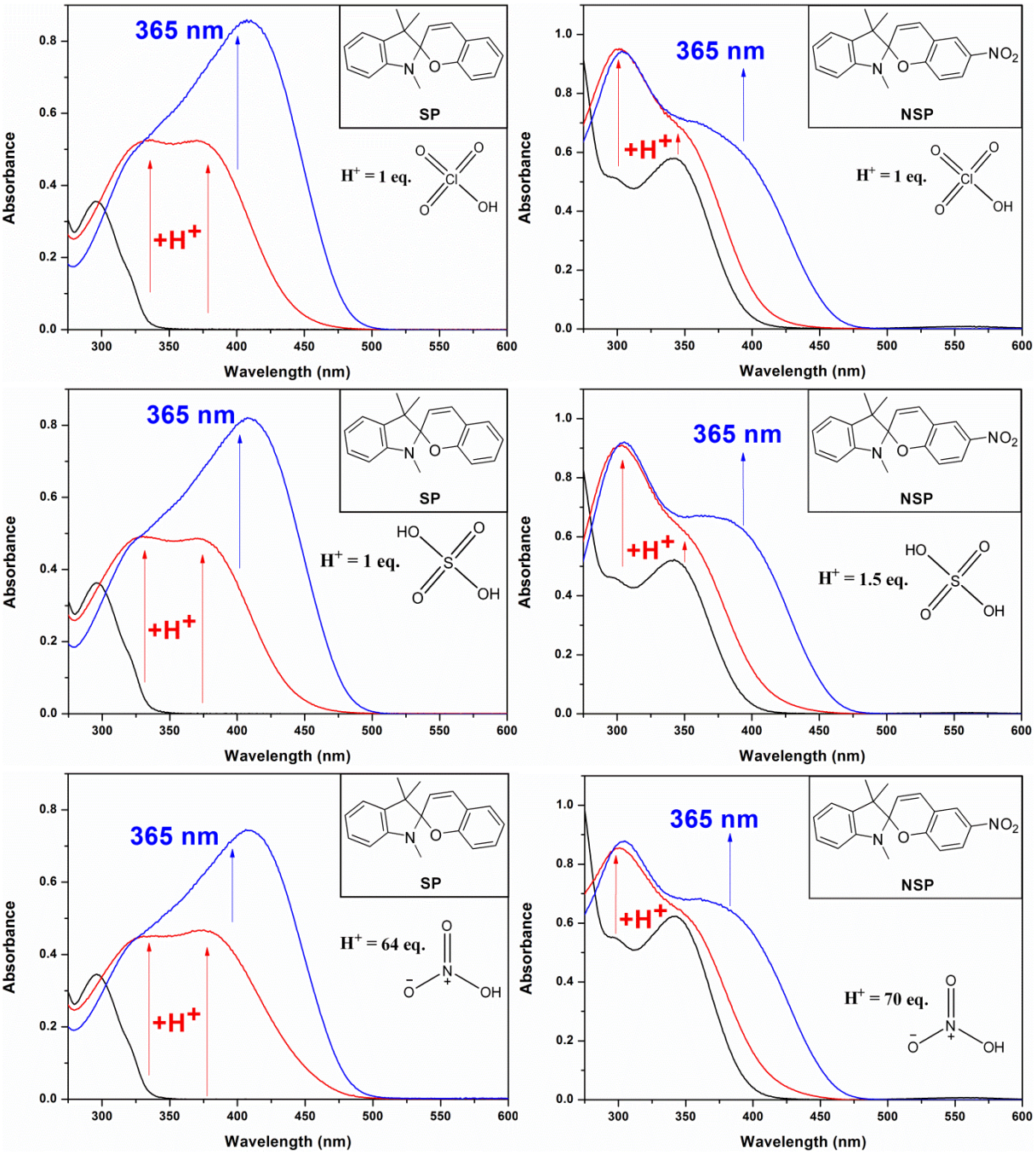


**Figure S3.** UV/vis absorption of (left column) **SP** and (right column) **NSP** (62 µM in acetonitrile, black lines), upon addition of the indicated proton source (red lines) and subsequent irradiation at 365 nm (blue lines). Reversion is again observed upon irradiation at 455 nm.

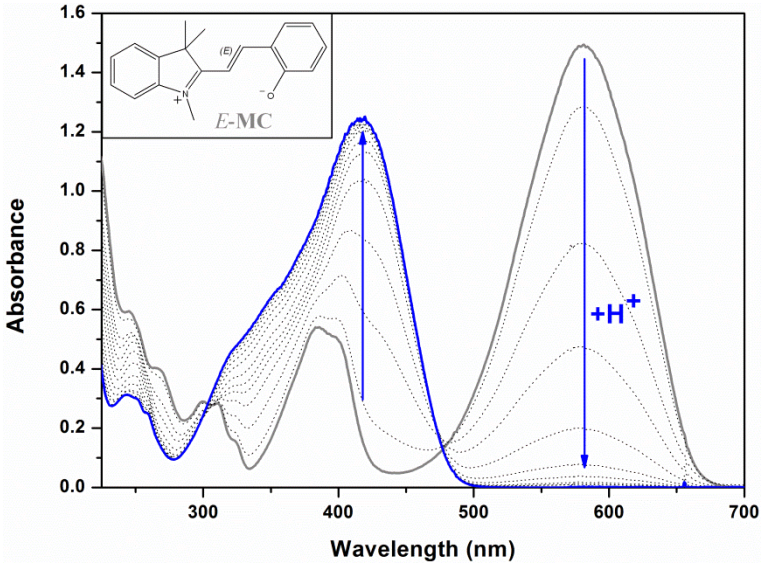


**Figure S4.** Low temperature UV/vis absorption of photoswitched **MC** from **SP** (-30 °C, 62 mM in acetonitrile, $\lambda_{exc}$ 300 nm, grey solid line) with addition of 150 nmol trifluoromethanesulfonic acid (to blue solid).

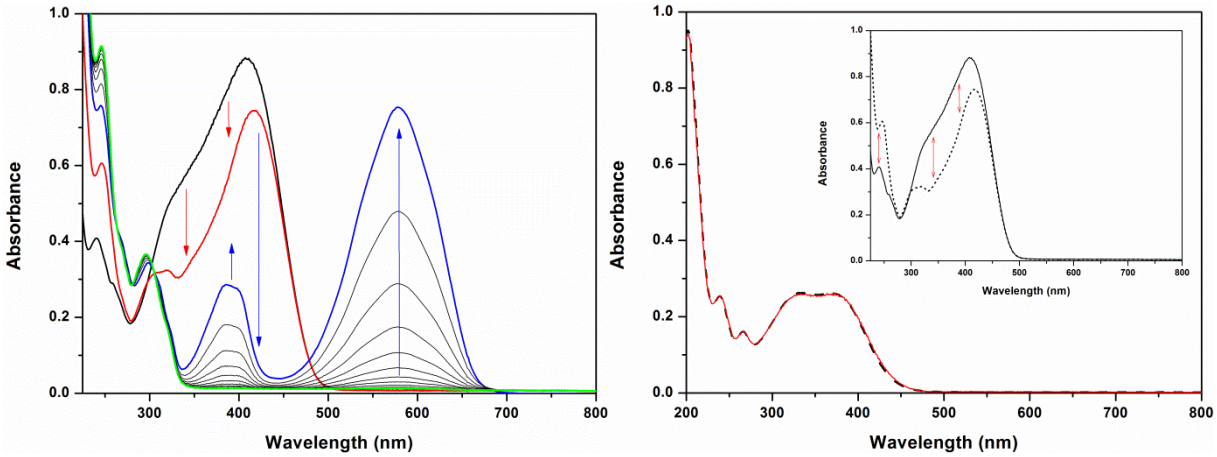


**Figure S5.** (Left) UV/vis absorption of **SP** (62 mM in acetonitrile, black solid line) after the previous pH-gated (300 nmol trifluoromethanesulfonic acid) photoconversion at 365 nm, while adding a first portion of 600 nmol NaOAc in 20 µL 9:1 acetonitrile/water (to red line, red arrows indicate direction of change), and a second equal portion (to blue line, blue arrows indicate direction of change), followed by swift thermal relaxation to the original spiropyran form (green line). (Right) (Inset) UV/vis absorption of **SP** (62 mM in acetonitrile, black solid line) after the previous pH-gated (300 nmol trifluoromethanesulfonic acid) photoconversion at 365 nm, while adding a first portion of 600 nmol NaOAc in 20 µL 9:1 acetonitrile/water. As deprotonated **SP** is formed the difference spectrum is "compensated" with 0.48 equivalents of the original closed form absorption, at which point the corrected differential absorption (solid red line) matches that of the protonated form (dashed black) precisely.

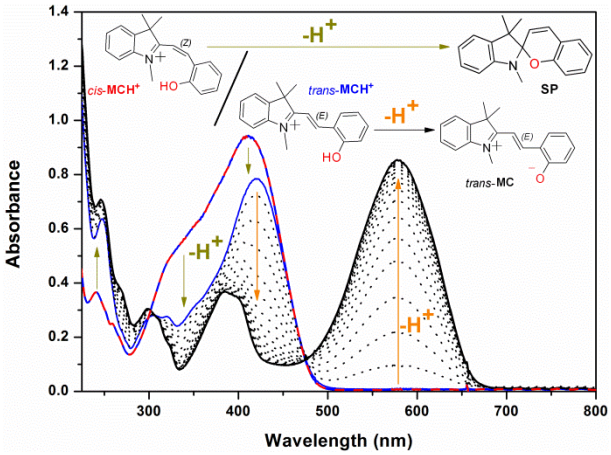


**Figure S6.** Low temperature UV/vis absorption of a mixture of *Z*- and *E*-isomer of **MCH**$^+$ (-30 °C, 62 mM in acetonitrile, red and blue alternatingly dashed line) after reaching the PSS in pH-gated photochromism with 150 nmol trifluoromethanesulfonic acid (1.2 equivalents, $\lambda_{exc}$ = 365 nm), while adding a first portion of 450 nmol NaOAc in 15 µL 9:1 acetonitrile/water (to solid blue line, green arrows indicate direction of change), and a second portion of 300 nmol NaOAc (to black line, yellow arrows indicate direction of change). Afterwards slow thermal relaxation back to the original closed spiropyran form is observed.

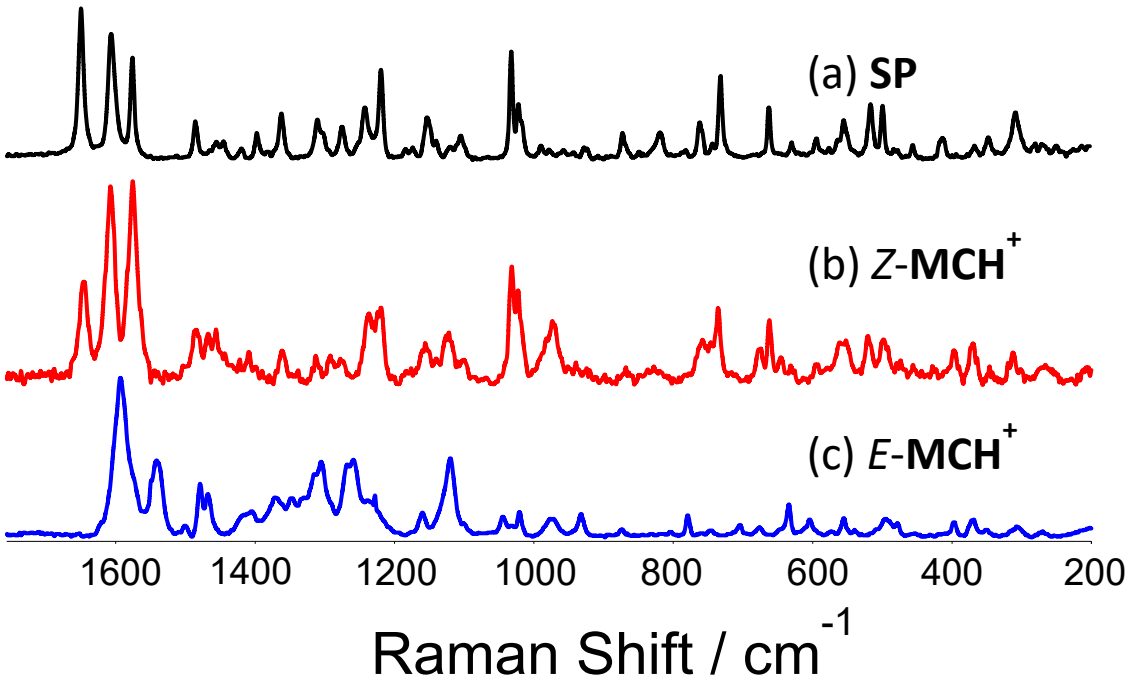

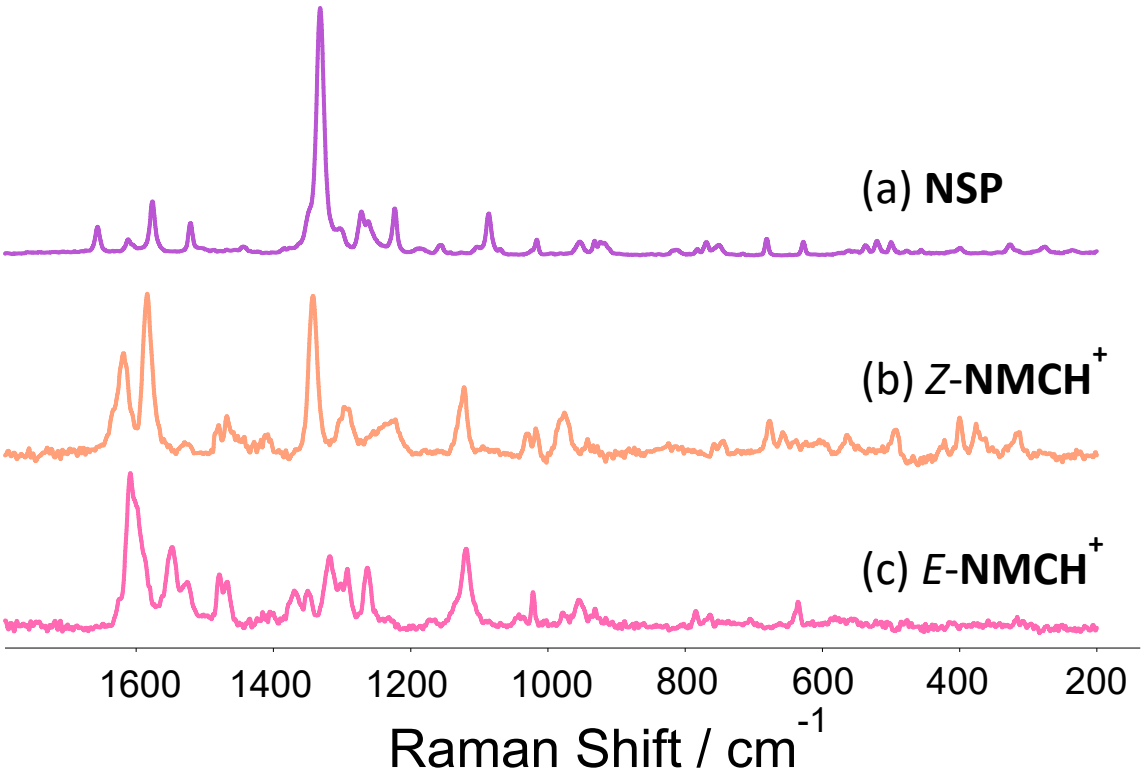


**Figure S7.** Experimentally obtained Raman spectra ($\lambda_{exc}$ 785 nm) of thin dropcast films of (top) **SP**, *Z*-**MCH**$^+$ and *E*-**MCH**$^+$ and (bottom) **NSP**, *Z*-**NMCH**$^+$ and *E*-**NMCH**$^+$. The dropcast films were prepared by casting a drop of saturated solution (in dichloromethane, [**N**]**SP**; as is, *Z*-[**N**]**MCH**$^+$; addition of 2 equiv. trifluoromethanesulfonic acid, *E*-[**N**]**MCH**$^+$; subsequent irradiation at 365 nm and scaled subtraction of the *Z* form) into a quartz crucible, allowing the volatile solvent to evaporate swiftly while leaving a thin solid film behind.

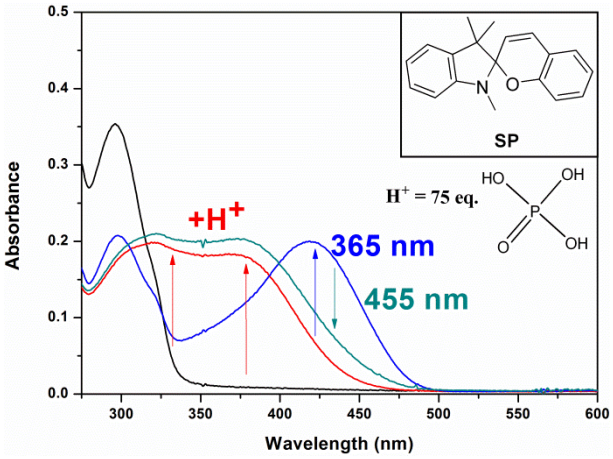


**Figure S8.** UV/vis absorption of **SP** (62 µM in acetonitrile, black line), upon addition of a large excess 75 equiv. $H_3PO_4$ (red line) and subsequent irradiation at 365 nm (blue line). Reversion occurs upon irradiation at 455 nm (cyan line).

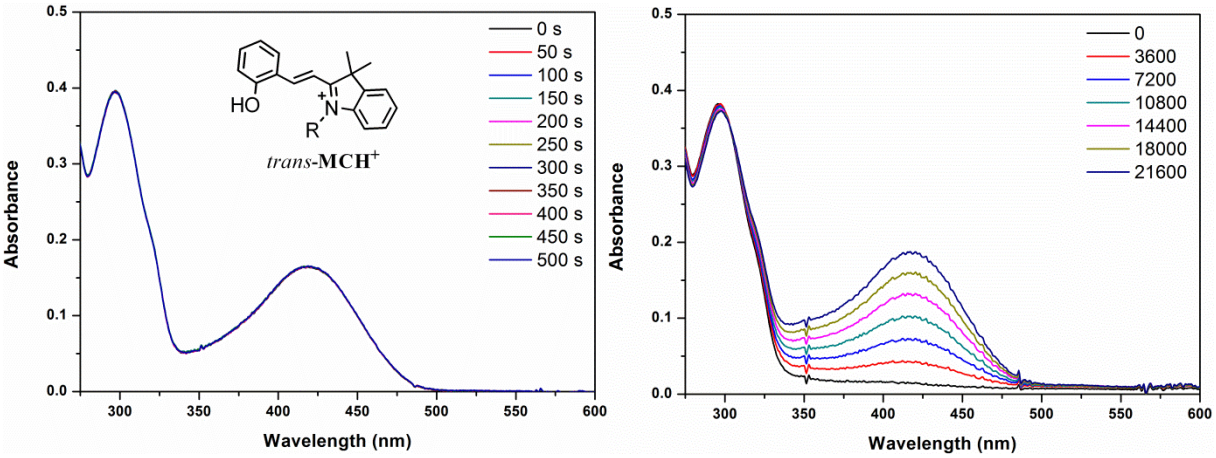


**Figure S9.** (Left) UV/vis absorption of *E*-**MCH**$^+$ (an estimated concentration of 9 µM by absorption versus the absorption of *E*-**MCH**$^+$ following direct protonation by triflic acid of the photoproduced **MC** form, **Figure S4**) resulting from addition of 1 equivalent of $H_3PO_4$ to 62 µM **SP** and subsequent irradiation at 300 nm to the PSS. Though the *E*-**MCH**$^+$ form is thermally more stable, attested by complete thermal conversion over time as seen in the NMR spectroscopy, its contribution to absorbing of incident light is deemed to result in this photostationary state. (Right) UV/vis absorption spectra of equimolar **SP** and phosphoric acid (62 µM in acetonitrile, black line) over several hours, showing thermal conversion to the *trans*-**MCH**$^+$ form over time.

**Theoretical methods.**

All our theoretical calculations have been performed with the Gaussian16.A03 code,[3] using default approaches, algorithms and thresholds, except when noted below. We have followed a computational protocol similar to the one proposed by Bieske,[4] though we accounted for solvent effects systematically using the Polarizable Continuum Model (acetonitrile). We performed DFT geometry optimization and vibrational frequency calculations with the PW6B95-D3 exchange-correlation functional[5] combined with the *def2*-TZVP atomic basis set for all atoms. These calculations were performed with the so-called *ultrafine* DFT integration grid, and used improved SCF convergence ($10^{-10}$ au, fully accurate integrals throughout) and geometry optimization ($10^{-5}$ au on rms forces, so-called "tight" criterion in Gaussian16) thresholds. For determining the various transition-states, we started with reasonable guesses and used the Berny algorithm with analytic determination of the Hessian at each point. It was checked at the end of the calculation that the obtained (single) imaginary frequency indeed corresponds to a chemically-sound displacement. For all transition states reported in the manuscript, we attempted calculations with both a normal and a so-called broken-symmetry wavefunction, but the latter systematically led back to the same solution during the SCF cycles. Discussion about the merits and limitations of the selected approach for TS determination can be found in the above-mentioned Bieske work. It should be underlined that our goal here was not to obtain quantitative estimates for all TS energies, but rather to compare four different chemically-related systems. The optical properties were explored with TD-DFT using the CAM-B3LYP[6] range-separated functional and the *aug*-cc-pVDZ atomic basis set. The vertical approximation was applied, so that one typically expects blue-shifted results as compared to experiment (in which vibronic couplings are present).

**TD-DFT characterizations.**

The Table below lists selected transition wavelengths and corresponding oscillator strengths computed for some key species.

**Table S1**. Computed vertical transition energies (expressed in nm) and corresponding oscillator strengths for selected dipole-allowed excited-states

| Species | λ (nm) | f | Species | λ (nm) | f |
|---|---|---|---|---|---|
| **SP** | 281 | 0.14 | **NSP** | 313 | 0.29 |
| *Z*-**MC** (CCC) | 458 | 0.31 | *Z*-**NMC** (CCC) | 427 | 0.46 |
| | 356 | 0.11 | | 344 | 0.36 |
| | 315 | 0.31 | | | |
| *E*-**MC** (TTT) | 478 | 0.87 | *E*-**NMC** (TTC) | 445 | 1.07 |
| | 325 | 0.30 | | 331 | 0.21 |
| | | | | 308 | 0.41 |
| **SPH$^+$** | 268 | 0.21 | **NSPH$^+$** | 285 | 0.14 |
| | 244 | 0.19 | | | |
| *Z*-**MCH$^+$** (CCT) | 358 | 0.44 | *Z*-**NMCH$^+$** (CCT) | 336 | 0.41 |
| | | | | 287 | 0.14 |
| | | | | 281 | 0.11 |
| *E*-**MCH$^+$** (TTT) | 390 | 1.08 | *E*-**NMCH$^+$** (TTT) | 377 | 1.08 |
| | 317 | 0.11 | | 283 | 0.23 |

[3] M. J. Frisch and co-corkers, Gaussian 16.A03, Gaussian Inc., Wallingford, CT, 2016.
[4] Markworth, P. B.; Adamson, B. D.; Coughlan, N. J. A.; Goerigk, L.; Bieske, E. J. *Phys. Chem. Chem. Phys.* **2015**, *17*, 25676..
[5] Zhao, Y.; Truhlar, D. G. *J. Phys. Chem. A* **2005**, *109*, 5656.
[6] Yanai, T.; Tew, D.; Handy, N. C. *Chem. Phys. Lett.* **2004**, *393*, 51.

**Theoretically determined Raman spectra.**

Below are presented the theoretically computed Raman spectra (normalized intensities but no scaling of the frequencies). These graphs can be straightforwardly compared to their experimental counterparts of **Figure S7**. One notices a reasonably good agreement in all cases, e.g., the **SP** isomer presents three intense bands of decreasing height at ca. 1600 $cm^{-1}$; whereas the most intense peak is located at small (large) wavenumbers in the *Z* (*E*) isomers of the protonated structures. One also notices that the impact of introducing a nitro group is strong for the closed isomer but more modest for the merocyanine structures, which also fits the measurements.

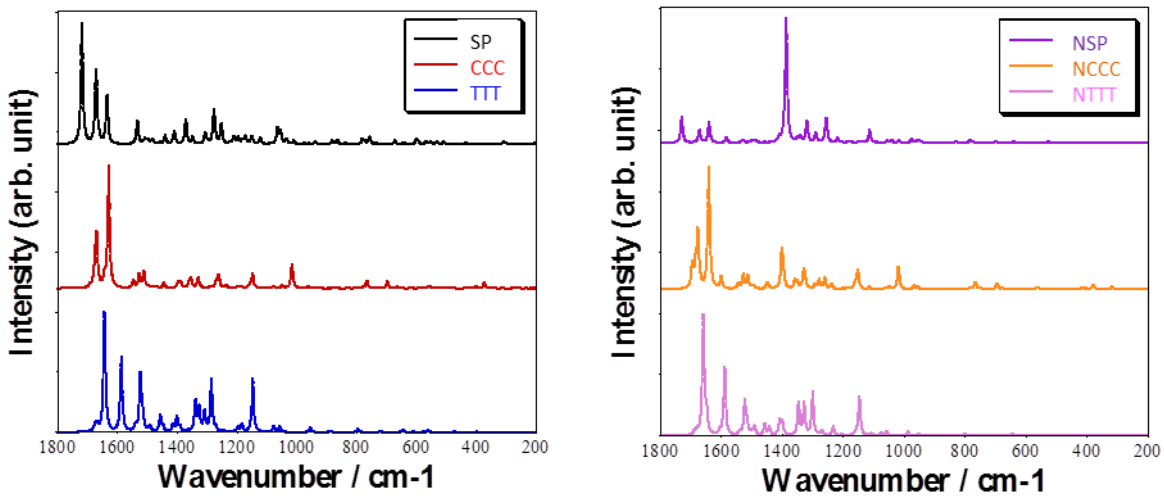


**Figure S10.** (Left) DFT computed Raman Spectra for **SP** and the protonated forms of *Z*-**MCH**$^+$ (CCC) and *E*-**MCH**$^+$ (TTT). (Right) Same information for the nitro derivatives.